Applied Radiation and Isotopes 146 (2019) 10–17

Contents lists available at ScienceDirect

Applied Radiation and Isotopes

journal homepage: www.elsevier.com/locate/apradiso

Cross sections for formation of ^{139m}Ce radioisotope through the ^{140}Ce (n, 2n) reaction over 13.73–14.77 MeV neutrons

Vishal D. Bharud[a], F.M.D. Attar[b], S.S. Dahiwale[a], S.D. Dhole[a], V.N. Bhoraskar[a,*]

[a] Department of Physics, Savitribai Phule Pune University, Pune 411007, India
[b] Poona College, K.B. H. Road, Pune 411001, India

HIGHLIGHTS

- Fast neutron induced (n, 2n) reaction cross sections of rare earth isotope ^{140}Ce for the formation of ^{139m}Ce, were measured.
- The neutron energies used were 14.77, 14.68, 14.42, 14.07 and 13.73 MeV neutron energies.
- The experimental cross sections were measured relative to ^{27}Al(n, p)^{27}Mg reaction.
- Cross sections estimated by EMPIRE-3.2 and TALYS-1.8 codes are in good agreement with the experimental cross sections.

ARTICLE INFO

Keywords:
^{140}Ce(n
2n)^{139m}Ce reaction cross sections
D + T reaction neutron
Activation and off-line γ-ray spectrometry
TALYS 1.8
EMPIRE-3.2 Malta

ABSTRACT

Cross sections for the formation of metastable state of ^{139}Ce through ^{140}Ce(n, 2n)^{139m}Ce reaction were measured at five neutron energies over 13.73–14.77 MeV range using the activation method and off-line gamma-ray spectrometric technique. These cross sections were in agreement with the corresponding theoretical cross sections estimated over 10–20 MeV neutrons by EMPIRE-3.2 code, using LEVEDEN 4 and strength function GSTRFN 0 parameters, and TALYS-1.8 code using ldmodel 5 and preeqmode 4 parameters. The estimated most probable excitation energies of ^{139}Ce were 1.320–3.877 MeV, respectively over 13.73 MeV and 14.77 MeV neutron energies.

1. Introduction

Studies of nuclear reactions induced by neutrons, gamma-rays and charged particles are important for obtaining information about the excited states and ground states of nuclei, in addition to nuclear reaction mechanisms (Naik et al., 2013; Şahan et al., 2016; Semkova et al., 2004; Vogt et al., 2002). Usually neutrons are produced from the D + D, D + T, ^{3}H(p, n), ^{7}Li(p, n) and ^{9}Be(p, n) reactions. Neutrons are also produced. Neutrons are also produced through gamma-ray induced reaction such as (γ, n) reaction in which normally electrons are used to generate bremsstrahlungradiation (Jagtap et al., 2016; Patil et al., 2012, 2010). For the neutron induced reactions, the cross-section data for a large number of nuclear reactions such as (n,n′), (n, 2n), (n, p) and (n, α) have been measured over a large energy range from threshold to 20 MeV and reported in the literature (Attar et al., 2014, 2008; Badwar et al., 2016; Lalremruata et al., 2012, 2009; Luo et al., 2009; Barough et al., 2014; Pandey et al., 2014; Yiğit, 2018). In some of the nuclear reactions, the excited nucleus decays to a metastable state, having a life–time in the range of milliseconds to a few hours, and then makes the transition to the ground state. Moreover, in some cases the excited nucleus has two channels through which it decays to the ground state, one directly and the other through the metastable state. Similarly, the ground state can also be radioactive, and therefore the contribution of the metastable state in the formation of the ground state is important (Kestelman et al., 2007; Luo et al., 2007; Parashari et al., 2018; Sarkar, Bhoraskar, 1992).

The cross sections for formation of metastable states can provide information on nuclear structure, spin distribution factor, nuclear level density and spin of energy levels. For an excited nucleus, the probabilities for decaying to the metastable state and to the ground state depend on the spin distribution factor. An approximate value of the cross section for the formation of metastable state can be therefore estimated from the spin distribution factor which is related to nuclear level density through a relation involving spin of nuclear levels, as described in our earlier publication (Sarkar and Bhoraskar, 1998).

The metastable state decays to a certain energy level or ground state

* Corresponding author.
E-mail address: vnb@physics.unipune.ac.in (V.N. Bhoraskar).

https://doi.org/10.1016/j.apradiso.2019.01.003
Received 18 September 2018; Received in revised form 5 January 2019; Accepted 10 January 2019
Available online 11 January 2019
0969-8043/

by emitting gamma-rays and may have a life-time in the range of milliseconds to a few hours. The cross section for the formation of a metastable state depends on the threshold of the particular nuclear reactions, energy of the incident neutrons and spins of the excited levels of the nucleus (Naylor and White, 1977; Yoshimi et al., 1998). The cross sections for the formation of a metastable state vary with the excitation energy of the nucleus, being produced by different nuclear reactions with suitable target nuclei. This study is important from the point of view of a basic understanding of the channel effects in the formation of metastable states of the nucleus. For fusion reactor technology extensive experimental data on low and high energy neutron-induced reactions have been evaluated and compiled (EXFOR, 2013). The rare-earth elements are always present in small concentrations in the structural material of the nuclear reactor. However, it has been observed that not much work has been carried out to study the cross-sections for the formation of a metastable state through the (n, 2n) reaction for rare earth elements (Bramlitt and Fink, 1963; Kong et al., 1998; Qaim, 1974; Van Gosen et al., 2014; Wille and Fink, 1960).

Among all the natural rare-earth elements, cerium has a relatively large abundance. Cerium is used with uranium oxide as a nuclear fuel for nuclear power in space (Katalenich et al., 2013). Cerium is also used as a radiation- hardening agent in the glass industry and as a diluent in uranium, plutonium and thorium oxide nuclear fuels due to its low neutron -capture cross- section. In nature it occurs as a silvery-white metal in the composition of oxides and chlorides. So far thirty five isotopes of cerium have been discovered, out of which four are stable and thirty one are unstable. The stable isotopes are ^{136}Ce, ^{138}Ce, ^{140}Ce and ^{142}Ce with isotopic abundances of 0.185(2)%, 0.251(2)%, 88.45(51)% and 11.11(51)%, respectively (Berglund and Wieser, 2011; Rosman and Taylor, 1998; Torrel and Krane, 2012).

A literature survey indicates that the cross sections of the ^{140}Ce(n, 2n)^{139m}Ce reaction over the neutron energy range of 13.4–14.95 MeV have been measured by a few researchers (Luo et al., 2015; Reyhancan et al., 2003; Sakane et al., 2001; Kasugai and Ikeda, 1997; Satoh et al., 1995). However, there are disagreements over the measurements of these cross- sections. So it is important to study the neutron- induced reactions for such rare- earth elements, and to improve the values of the cross sections with known, systematic uncertainties.

In the present work, the cross-sections for the formation of ^{139m}Ce through the reaction ^{140}Ce(n, 2n)^{139m}Ce over the neutron energy range of 13.73–14.77 MeV have been measured by using activation method and employing a (D-T) reaction based 14 MeV Neutron Generator. The nuclear reaction yields are obtained by absolute measurements of the gamma activities of the product nuclei using a high-purity germanium detector. For this reaction, the theoretical values of the cross sections have been estimated by using the TALYS 1.8 (Koning et al., 2015) and EMPIRE-3.2 Malta (Herman et al., 2013) computer codes. This reaction has threshold energy of 10 MeV and is therefore useful for studying nuclear reactions at neutron energies higher than 10 MeV without any interference from low energy neutrons. The measured cross sections have been compared with the respective theoretical cross-sections, as well as with the experimental cross-sections measured earlier and reported in the nuclear data center library such as the Evaluated Nuclear Data File (ENDF/B-VII.1, 2018.) (ENDF) and Experimental Nuclear Reaction Data (Otuka and Smith, 2014) (EXFOR).

2. Experimental details

2.1. Neutron irradiation

The neutron irradiation work was carried out using the 14 MeV Neutron Generator facility of the Department of Physics, Savitribai Phule Pune University, Pune, India, in which neutrons are produced through D-T reaction. For the measurement of ^{140}Ce(n, 2n)^{139m}Ce reaction cross section, each sample was made by packing a mixture of natural $CeCl_3$(99.99%) powder and thin pieces of aluminum foil (99.99%), of total weight of ~ 1.5 g, in a polythene bag. By folding the polythene bag the cerium-aluminum sample of size ~ 10 mm × 10 mm × 3 mm was obtained. Following the same procedure, twenty samples were prepared, and divided in three groups, such that each group had five samples. The remaining five samples were used for deciding the neutron irradiation time. The samples of three groups were used for the measurement of cross sections of ^{140}Ce(n, 2n)^{139m}Ce reaction with ^{27}Al (n, p)^{27}Mg as a monitor reaction.

The half life of ^{139m}Ce is 57.58 s (Joshi et al., 2016) whereas that of monitor ^{27}Mg is 9.458 min (Basunia, 2011). To decide an optimum neutron irradiation period, five samples were irradiated with 14.77 MeV neutrons one each for 600, 500, 400, 300 and 240 s. The gamma-ray activity of ^{139m}Ce was found to saturate for neutron irradiation time 300 s and above. It was therefore decided to use irradiation period of 240 s for which gamma-ray activities of both ^{139m}Ce and ^{27}Mg were adequate for the present experiment.

For the neutron irradiation experiment, a semicircular aluminum ring of 50 mm radius was horizontally fixed around the tritium target holder in such way that the axis of the semicircular ring, was perpendicular to ground, passing through the tritium target. Angles from 0° to 120° were marked on the ring for the identification of angular positions of 0°, 30°, 60°, 90° and 120° with the reference to center of tritium target. Five samples of one set were mounted on aluminum ring in a such way that one sample was fixed at one angular position respectively at 0°, 30°, 60°, 90° and 120° marked on the ring. The 14.77 MeV neutrons were produced by bombarding ~175 keV deuterium ions, of beam diameter ~4 mm and ~100 μA, on an 8 Ci tritium target. The neutron flux measured by an aluminum foil near the tritium target was ~ 10^8n/cm^2 s. All the five mounted samples were irradiated simultaneously with neutrons for 240 s, but with different energy of neutrons. As per the energy distribution of the emitted neutrons, the samples mounted at 0°, 30°, 60°, 90° and 120° angular position were irradiated with 14.77 MeV, 14.68 MeV, 14.42 MeV, 14.07 MeV and 13.73 MeV energy of neutrons, respectively (Attar et al., 2008; RNAL, 2002). After the completion of the irradiation period of 240 s, the neutron generator was switched off and all the five samples were taken out and transferred to the gamma-ray counting room. The Table 1 gives details of the nuclear decay data of the ^{139m}Ce and ^{27}Mg radioisotopes produced through the ^{140}Ce(n, 2n)^{139m}Ce and ^{27}Al(n, p)^{27}Mg reactions, respectively (Basunia, 2011; Joshi et al., 2016).

Following the same experiment procedure, a set of five samples of second group and a set of five samples of third group were irradiated with neutrons of different energies under identical conditions. The details of the activation cycle such as neutron energies, irradiation period, gamma-rays counting period, cooling period and angular positions of the five samples during neutron irradiation are given in Table 2.

Table 1
Nuclear data for ^{139m}Ce and ^{27}Mg radioisotopes.

Nuclear Reaction	Isotopic Abundance(%)	Reaction Product	Half life	E_γ (keV)	Gamma-Ray Abundance (%)	Reference
^{140}Ce(n, 2n)	88.450(51)	^{139m}Ce	57.58 s (32)	754.24	92.6	(Joshi et al., 2016)
^{27}Al(n, p)	100	^{27}Mg	9.458 m (12)	843.76	70.94(9)	(Basunia, 2011)
				1014.52	29.06(9)	(Basunia, 2011)

Table 2
Details of the activation cycle and angular positions of the samples during neutron irradiation.

Angular Position	Neutron Energy (MeV)	Irradiation time (t_1) (s)	Cooling time (t_2) (s)	Counting time (t_3) (s)
0	14.77(17)	240	30	40
30	14.68(15)	240	80	40
60	14.42(12)	240	130	40
90	14.07(8)	240	180	40
120	13.73(7)	240	230	40

2.2. Measurement of gamma-ray activity

The energy and activity of the gamma-rays emitted by each neutron irradiated sample were measured by a coaxial HPGe (38%) detector, cooled by LN2 cryostat. The gamma-ray spectrum was recorded by connecting the detector to a 4096 channel analyzer through amplifier, discriminator and other standard nuclear electronic units. To avoid contamination, the detector surface was covered with ~ 0.1 mm thick polyethylene sheet. A Canberra make Multi Gamma Standard MGS-3 source was used for the measurement of detection efficiency and also for energy calibration, using gamma-rays over the energy range of 88–1332 keV. The measured energy resolution of the HPGe detector was ~ 2.5 keV at 1332 keV gamma-rays of Co-60 source.

After neutron irradiation all the five samples were brought to gamma-ray counting room and sample irradiated at 0° angular position was mounted in front of HPGe detector for gamma-ray counting within a period of 30 s. In this manner the cooling time for the first sample was 30 s. After recording gamma-ray spectrum of the first sample by HPGe detector for 40 s, the sample was removed. The second sample irradiated at 30° was mounted in front of the HPGe detector and spectrum was recorded for 40 s. A time period of 10 s was required for removing the sample and mounting the other sample in front of the HPGe detector. Following the same procedure the gamma-ray spectra of samples irradiated 60°, 90° and 120° were recorded sequentially. In this manner, gamma–ray spectra of five samples of the first, the second and the third group were recorded by HPGe detector, the details of which are given in the Table 2. The spectrum of the background radiation was measured for 40 s and the recorded gamma-ray spectrum of each sample was corrected for the background radiation using a computer program. The recorded gamma-ray spectrum of a sample irradiated with neutrons at 0° angular position is shown in Fig. 1

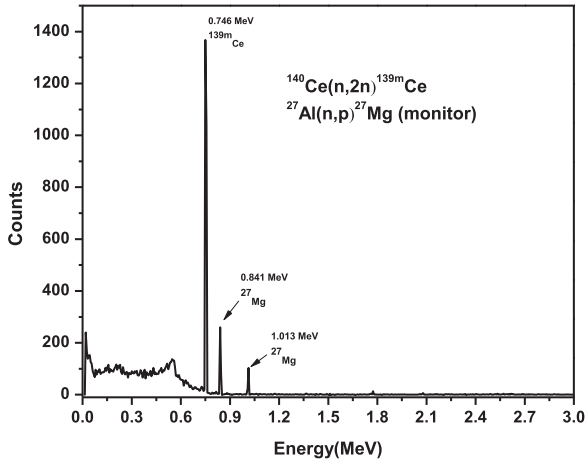

Fig. 1. Gamma-ray spectrum of the sample irradiated at 0^0 position with 14.77 MeV neutrons. The photo peaks of ^{139m}Ce and ^{27}Mg are indicated with energies.

2.3. Data analysis

Fig. 1 shows a typical recorded gamma-ray spectrum of ^{139m}Ce and ^{27}Mg radioisotopes produced by irradiating a sample of Ce and Al with 14.77 MeV neutrons. The activation cross sections for the ^{140}Ce (n,2n)^{139m}Ce reaction at 13.73 MeV, 14.07 MeV, 14.42 MeV, 14.68 MeV and 14.77 MeV neutron energies were estimated using the nuclear data given in Table 1 and the following activation expression(1) (Attar et al., 2008).

$$\sigma = \sigma_M \frac{A \varepsilon_M I_{\gamma M} \lambda}{A_M \varepsilon I_\gamma \lambda_M} \frac{N_M}{N} \frac{(1-e^{-\lambda M t1})}{(1-e^{-\lambda t1})} \frac{e^{-\lambda M t2}}{e^{-\lambda t2}} \frac{(1-e^{-\lambda M t3})}{(1-e^{-\lambda t3})} \quad (1)$$

In the above expression, σ is the reaction cross section, A is the number of counts under the photo peak, I_γ is photon disintegration probability, ε is the detector efficiency, σ is the cross section for the nuclear reaction, λ is the decay constant, N is the number of atoms of the isotope of the element, t_1 is the irradiation time, t_2 is the cooling time, and t_3 is the period for which the gamma-ray activity was measured. The quantity with the subscript M stands for the monitor element and reaction. For the monitor ^{27}Al(n, p)^{27}Mg reaction, the cross section used were 78.24, 73.65, 68.31, 66.31, 63.98 mb respective at 13.73 MeV, 14.07 MeV, 14.42 MeV, 14.68 MeV and 14.77 MeV neutron energies. These cross sections have been obtained from literature (Filtankov, 2016) and normalized with Evaluated Nuclear Data File (ENDF) data corresponding to specific neutron energies.

In expression (1), the uncertainty associated with the measurement of a parameter is independent of the uncertainty associated with each of the other parameters. The uncertainty, dσ, of cross section was estimated by the error analysis based on the quadrature method(Taylor, 1939) and using the following expression (2) from the literature (Otuka et al., 2017);

$$(\delta\sigma/\sigma)^2 = \sum_q (\delta q/q)^2 + \sum_q (\delta q_M/q_M)^2 + (\delta\sigma_M/\sigma_M)^2 + \sum_i (\delta t_i/t_i)^2 \quad (2)$$

where, q is for ^{139}Ce, q_M is for the monitor ^{27}Mg (q, q_M = A, ε, N, I, λ). Similarly, t_i is the uncertainty in the irradiation time t_1, cooling time t_2, counting time t_3. The uncertainty in the cross section of monitor reaction $\delta\sigma_M$ was obtained from literature (Taylor, 1939). The estimated uncertainties in the measured parameters are given in Table 3.

The above mentioned uncertainties were used for the estimation of experimental cross sectionsat each neutron energy.

3. Theoretical calculations

The cross sections of the ^{140}Ce(n, 2 n)^{139m}Ce reaction over the neutron energy range of 10–20 MeV were theoretically estimated using the TAYLS and EMPIRE computer codes. Two sets of calculations were performed in the framework of direct reaction, compound nucleus, pre-equilibrium emission and statistical Hauser-Feshbach models using TAYLS 1.8 (Koning et al., 2015) and EMPIRE-3.2 (Herman et al., 2013)

Table 3
Uncertainties in different parameters used in estimation of experimental cross sections of the^{140}Ce(n, 2n)^{139m}Ce reaction.

Parameters	Limit (%)
Counting rate	≤ 5–6
Efficiency calibration	≤ 4
Self- absorption	≤ 0.3
Neutron flux	≤ 6
Intensity I_γ	≤ 3
Irradiation time t_1	≤ 1
Cooling time t_2	≤ 1
Counting time t_3	≤ 1

The options of nuclear level density and nucleon potentials which yielded the values of theoretical cross-sections close to the respective experimental cross section measured in the present work were used.

3.1. Theoretical calculation using TALYS-1.8 code

Using TALYS-1.8 version of TENDL Library, the theoretical cross sections for the formation of metastable states of ^{139}Ce through the ^{140}Ce (n,2n) ^{139m}Ce reaction over 10–20 MeV neutron energies were estimated and compared with the experimental cross sections measured at five neutron energies in the present work as well as with the three sets of cross sections reported in literature (Reyhancan et al., 2003; Sakane et al., 2001; Kasugai and Ikeda, 1997) at five or more neutron energies. In addition, the theoretical cross sections for ^{140}Ce (n, n′) ^{140}Ce, ^{140}Ce(n, 2n)^{139}Ce and ^{140}Ce(n, 3n)^{138}Ce reactions were also estimated over 10–20 MeV neutron energy range

The required database was generated from the Reference Input Parameter Library RIPL (Capote et al., 2009). The global optical model potential parameterization of Koning and Delaroche (Koning and Delaroche, 2003), and the level density option ldmodel 5 were used. The microscopic level densities and the gamma strength functions were respectively obtained from Hillarie's combinatorial Tables (Hilaire et al., 2012), and data base available in literature (Gardner, 1984; Hauser and Feshbach, 1952; Kopecky, 1817). The contribution of the compound nucleus was calculated by using the Hauser-Feshbach model (Hauser and Feshbach, 1952).

In the present work the cross sections of ^{140}Ce(n, 2n)$^{139\,m}$Ce reaction were estimated by TALYS-1.8 code using the following six level density models (Koning et al., 2015);

(1) Level density model 1(LDM-1): The constant temperature model is used in the low excitation region and the Fermi-gas model is used in the high excitation energy region. The transition energy is around the neutron separation energy.
(2) Level density model 2(LDM-2): The back-shifted Fermi-gas model.
(3) Level density model 3(LDM-3): The generalized super-fluid model.
(4) Level density model 4(LDM-4): The microscopic level densities (Skyrme force) from Goriely'sTables (Goriely et al., 2008, 2001).
(5) Level density model 5(LDM-5): The microscopic level densities (Skyrme force) from Hilaire's combinatorial tables (Goriely et al., 2008, 2001).
(6) Level density model 6(LDM-6): The microscopic level densities (temperature-dependent Hartree- Fock-Bolyubov, Gogny force) from Hilaire's combinatorial Tables (Hilaire et al., 2012).

Similarly,the default basic input parameters used were as follows: projectile as neutron, element as cerium, mass number as 140, and neutron energy in terms of range file varying from 10 M to 20 MeV. In addition,(i) by enabling the prequilibrium mode, all the four preqmodes 1,2,3 and 4 and (ii) the gamma-ray transmission coefficients (Gardner, 1984) from 0 to 1 in a step of 0.10 were used. It was observed that the theoretical cross sections could be closer with the experimental cross–sections when preqmode-4 and gnorm parameter value of 0.2 were used for all the six level density models.

Using all these parameters as input to the TALYS-1.8 code,eight plots of theoretical cross sections were obtained over 10–20 MeV neutron energy range. As shown in Fig. 2,out the eight plots of cross sections, six plots were obtained by using six level density models, from ldmodel 1 to ldmodel 6. The remaining two plots were obtained by using default parameters with ldmodel 1 and then replacing ldmodel 1 by ldmodel2. The cross sections measured at five neutron energies in the present work, and three sets of cross sections reported in literature EXFOR data (Reyhancan et al., 2003; Sakane et al., 2001; Kasugai and Ikeda, 1997) for five or six neutron energies over the range of 13–15 MeV, were compared with these eight plots of theoretical cross sections given in Fig. 3. These eight plots of cross sections were

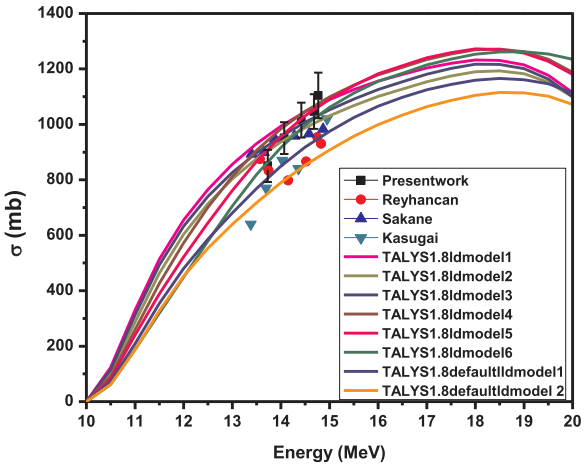

Fig. 2. Cross sections for^{140}Ce(n, 2n)^{139m}Ce reaction (i) in eight plots obtained theoretically by TALYS 1.8 over 10–20 MeV neutron energy range using pre-equilibrium, preeqmode 4 and parameters of level density model 1–6 and default ld model 1 & 2 (ii) measured in the present work at 13.73 MeV, 14.07 MeV, 14.42 MeV, 14.68 MeV and 14.77 MeV neutron energies and (iii) reported in literatrure by Reyhancan et al. (2003), Sakane et al. (2001) and Kasugai and Ikeda (1997)).

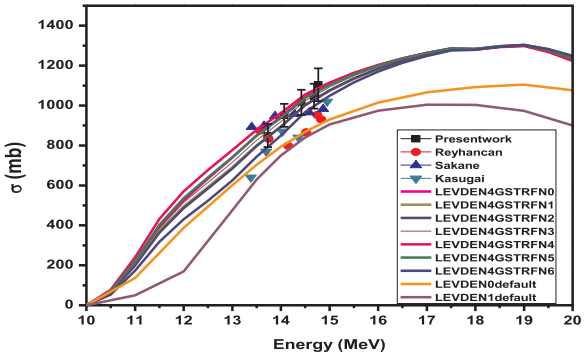

Fig. 3. Cross sections of ^{140}Ce(n, 2n)$^{139\,m}$Ce reaction(i) in nine plots theoretically obtained by EMPIRE 3.2 over 10–20 MeV neutron energy range using LEVEDEN 4 with parameters of GSTRFN from 1–6 and LEVDEN 0&1 default parameters(ii) measured in the present work at 14.07 MeV, 14.42 MeV, 14.68 MeV and 14.77 MeV neutron energies and (iii) reported in literatrure by Reyhancan et al. (2003), Sakane et al. (2001) and Kasugai and Ikeda, (1997).

obtained to encompass five values of experimental cross sections measured in the present work and three sets of cross sections reported in literature (Reyhancan et al., 2003; Sakane et al., 2001; Kasugai and Ikeda, 1997) at five or six neutron energies. It can be seen in Fig. 2 that all the five cross sections measured in the present work could be matched,with in experimental errors, with the theoretical plot obtained using ldmodel 5 parameter (Goriely et al., 2008).

3.2. Theoretical calculation using EMPIRE Code

Using the EMPIRE-3.2 nuclear code (Herman et al., 2013), the theoretical cross sections for the formation of metastable state of ^{139}Ce through ^{140}Ce (n,2n) $^{139\,m}$Ce reaction over 10–20 MeV neutron energies were estimated and compared with the experimental cross sections measured at five neutron energies in the present work as well as with the three sets of cross sections reported in literature (Reyhancan et al., 2003; Sakane et al., 2001; Kasugai and Ikeda, 1997) at five or more neutron energies.

The EMPIRE-3.2 nuclear code was used with the default parameters LEVDEN 0 and GSTRFN 1, over 10–20 MeV neutron energy range. The discrete levels were taken from the RIPL-3 level file, based on ENSDF

Table 4
For ^{140}Ce(n, 2n)^{139m}Ce reaction induced by 13.73–14.77 MeV neutrons, the most probable energies with which (i) the first neutron and the second neutron are emitted and (ii) the corresponding excitation energy of ^{139}Ce nucleus.

Neutron Energy [MeV]	Compound nucleus energy [MeV]	Most probable energy of the emitted first neutron [MeV]	Most probable energy of the emitted second neutron [MeV]	Excitation Energy of ^{139}Ce nuclei [MeV]
13.73	19.06	1.00	0.33	3.101
14.07	19.398	1.02	0.51	3.238
14.42	19.745	1.04	0.52	3.556
14.68	20.003	1.06	0.53	3.784
14.77	20.093	1.06	0.53	3.873

(Capote et al., 2009). In the EMPIRE-3.2 code,there are five nuclear level density (NLD) parameters (Herman et al., 2013) as given below;

(i) LEVDEN 0. EMPIRE NLD (EGSM RIPL-3) as default.
(ii) LEVDEN 1. Refitted GSM model (Ignatyuk) NLD.
(iii) LEVDEN 2. Refitted Gilbert & Cameron NLD.
(iv) LEVDEN 3. RIPL-3 HFB parity dependent NLD.
(v) LEVDEN 4. EMPIRE 2.18 Gilbert & Cameron NLD.

All these nuclear level density parameters are defined on the nuclear potential and threshold of the reaction under study. In the present work, the cross sections over 10–20 MeV neutron energy range were estimated by EMPIRE-3.2 code and using all the five nuclear level density parameters. The Gamma ray strength functions, GSTRFN, from 0 to 6,involving enhanced generalized, modified, mughabghab, and standard Lorentzian were obtained from RIPL and literature (Kopecky et al., 1993; Mughabghab and Dunford, 2000; Plujko, 2000).The nuclear level density LEVDEN 0 was used as the default with gamma-ray strength function GSTRFN 1 (Kopecky et al., 1993).Similarly, the nuclear level densities from LEVDEN 1 to LEVDEN 4 were used with all the seven GSTRFN varying from 0 to 6 (Mughabghab and Dunford, 2000; Plujko, 2000).

Nine plots of theoretical cross sections over 10–20 MeV neutron energy range estimated by EMPIRE-3.2 with different input parameters are shown in Fig. 3. For comparison, the cross sections measured in the present work at five neutron energies and three sets of cross sections reported in literature EXFORdata (Reyhancan et al., 2003; Sakane et al., 2001; Kasugai and Ikeda, 1997) are also given in Fig. 3.

Fig. 3 shows that these nine plots of theoretical cross sections have encompassed all the cross sections measured at five neutron energies in the present work and three sets of cross sections at five and more neutron energies reported in EXFOR data (Reyhancan et al., 2003; Sakane et al., 2001; Kasugai and Ikeda, 1997) in the range of 13–15 MeV.

3.3. Comparison of experimental and theoretical cross sections

The cross sections of ^{140}Ce(n, 2n)^{139m}Ce reaction(i) theoretically estimated over 10–20 MeV neutron energy range using (a) EMPIRE-3.2 –LEVEDEN 4 with parameters of GSTRFN 0 and (b) TALYS-1.8 ldmodel 5 are plotted in Fig. 5. In addition,Fig. 5 also shows experimental cross sections (i) measured in the present work at 13.73 MeV 14.07 MeV, 14.42 MeV, 14.68 MeV and 14.77 MeV neutron energies and (ii) reported in literatrure EXFOR data by Reyhancan et al. (2003),Sakane et al. (2001) and Kasugai and Ikeda (1997). Results shown in Fig. 5 give a comparison between the theoretical cross sections with the experimental cross sections measured in the present work as well as reported in EXFOR data (Reyhancan et al., 2003; Sakane et al., 2001; Kasugai and Ikeda, 1997).

3.4. Estimation of other cross sections

For comparison, the cross sections of ^{140}Ce (n, n′) ^{140*}Ce, ^{140}Ce (n, 2n) ^{139}Ce and ^{140}Ce (n, 3n) ^{138}Ce reactions over 10–20 MeV neutron energy range were also estimated using TALYS 1.8 code and the results are given in Fig. 5.

3.5. Excitation energy of ^{139}Ce

In the ^{140}Ce (n, 2n) ^{139}Ce reaction the cross section for the formation of metastable state, ^{139m}Ce, is decided by the most probable energy of excitation of ^{139}Ce.For this reaction,the most probable energy of excitation of ^{139}Ce was estimated by considering the energies with which the first neutron and the second neutron are emitted, at a given incident neutron energy. For five incident neutron energies over the neutron energy range of 13.73–14.77 MeV, the most probable excitation energies of the ^{139}Ce were estimated using the EMPIRE-3.2 code and the results are given in Table 4.

4. Results and discussion

The cross sections of ^{140}Ce(n, 2n)^{139m}Ce reaction (i) over the neutron energy range of 13.73–14.77 MeV have been measured and (ii) theoretically estimated using TALYS-1.8 and EMPIRE-3.2 codes over the neutron energy range of 10–20 MeV. Fig. 1 shows the gamma-ray spectrum of the Ce-Al sample irradiated with 14.77 MeV neutrons. The photo-peaks at 0.754 MeV due to ^{139m}Ce and that at 0.841 MeV and 1.013 MeV due to ^{27}Mg radioisotopes have clearly appeared in the recorded gamma-ray spectrum. The photo peaks at the same energies were also present in the gamma-ray spectra of other Ce-Al samples placed at different angular positions and irradiated with neutrons of different energies. These results show that over the neutron energy range of 13.73–14.77 MeV, both cerium and aluminum elements could be activated and the intensities of the recorded photo peaks were good enough for the estimation of cross sections. It is observed in Table 4 that at an incident neutron of 14.77 MeV energy, the most probable excitation energy of ^{139}Ce is 3.873 MeV, which is closer to the first excited energy level of 3.877 MeV (Joshi et al., 2016).For $^{139\,m}$Ce, the half life of 57.58 s was used for estimation of experimental cross sections, whereas half life of 54.8 s was considered based on RIPL data for estimation of theoretical cross sections using TALYS-1.8 (Koning et al., 2015) and EMPIRE-3.2 (Herman et al., 2013)codes. However, the theoretically estimated cross sections did not change when the half-life of 57.58 s or 54.8 s was used.

From Table 5, it is observed that the measured cross sections for the formation of metastable state of ^{139}Ce varies from 850 ± 58 mb to 1092 ± 81 mb over 13.73–14.77 MeV neutron energy range.In literature,experimental cross sections for the ^{140}Ce(n, 2n)$^{139\,m}$Ce reaction over 13.4–14.95 MeV neutron energy range have been reported (Luo et al., 2015; Reyhancan et al., 2003; Sakane et al., 2001; Kasugai and Ikeda 1997). However, the cross sections reported in literature (Luo et al., 2015; Reyhancan et al., 2003; Sakane et al., 2001; Kasugai and Ikeda, 1997)at five or six neutron energies over 13.4–14.95 MeV range were only used for comparison with the cross sections measured at five neutron energies in the present work.

Fig. 3 shows plots of theoretical cross sections of ^{140}Ce(n, 2n)^{139m}Ce reaction over 10–20 MeV neutron energy range,estimated theoretically using TALYS 1.8 code with different values of level densities

Table 5
Cross sections of ^{140}Ce(n, 2n)^{139m}Ce nuclear reaction (i) measured in the present work over the range of 13.73–14.77 MeV neutron energies [9], (ii) theoretical values estimated from TALYS 1.8 and EMPIRE 3.2 codes and (iii) literature values from references (Reyhancan et al., 2003; Sakane et al., 2001; Kasugai and Ikeda, 1997).

Neutron Energy (MeV)	Present work σ (mb)	Theoretical σ (mb)		Neutron Energy (MeV)	Sakane et al. σ (mb)	Neutron Energy (MeV)	Kasugai et al. σ (mb)	Neutron Energy (MeV)	Reyhancan et al. σ(mb)
		TALYS-1.8	EMPIRE3.2						
13.73(7)	850 ± 58	914	895	13.40(5)	893 ± 38.39	13.38	640 ± 30	13.57	875
14.07(8)	951 ± 58	964	970	13.65(5)	899 ± 38.65	13.7	770 ± 30	13.75	833
14.42(12)	1015 ± 63	1020	1016	13.88(5)	948 ± 40.76	14.03	870 ± 40	14.15	798
14.68(15)	1047 ± 62	1052	1072	14.28(5)	958 ± 41.19	14.36	840 ± 40	14.52	866
14.77(17)	1092 ± 81	1060	1079	14.58(5)	966 ± 41.53	14.95	1020 ± 40	14.75	953
–	–	–	–	14.87(5)	983 ± 42.26	–	–	14.83	930

corresponding to model 1 to model 6. In addition, Fig. 3 shows the cross sections for ^{140}Ce(n, 2n)^{139m}Ce reaction (i) measured in the present work at 13.4 MeV, 14.07 MeV, 14.42 MeV, 14.68 MeV and 14.77 MeV neutron energies and (iii) reported in literature Reyhancan et al. (2003), Sakane et al. (2001) and Kasugai and Ikeda (1997) for comparison.

It can be observed in Fig. 2 that all the five values of cross sections measured in the present work are covered under the six theoretical plots obtained by TALYS 1.8 using preequilibrium, preeqmode and parameters of level density models 1–6. However, only a few values of cross sections of the three sets of cross sections reported in literature (Reyhancan et al., 2003; Sakane et al., 2001; Kasugai and Ikeda, 1997) show matching with these six plots given in Fig. 2. A detailed analysis of Fig. 2 shows that (i) out of six cross sections reported by Reyhancan et al. (2003), only two cross sections at 13.57 MeV and 13.75 MeV neutron energies (ii) out of five cross sections reported by Kasugai and Ikeda (1997) only one cross section at 14.95 MeV neutron energy, and (iii) out of six cross sections reported by Sakane et al. (2001), four cross sections at 13.40,13.65,13.88 and 14.28 MeV neutron energies lie on these six plots of theoretical cross sections. However,all the cross sections reported in literature (Reyhancan et al., 2003; Sakane et al., 2001; Kasugai and Ikeda, 1997), could be covered when two additional plots of cross sections estimated by TALYS-1.8 using default ldmodel 1 & 2 were plotted in Fig. 2. It can be observed in Fig. 2 that all the literature values of experimental cross sections (Reyhancan et al., 2003; Sakane et al., 2001; Kasugai and Ikeda, 1997) in addition to the five cross sections measured in the present work are encompassed by the eight plots of theoretical cross sections estimated by TALYS-1.8,with different input parameters.

While comparing the three sets of cross sections reported in literature with the plots in Fig. 3,it is observed that (i) out of six values of cross sections reported by Reyhancan et al. (2003), only two values of cross sections at 13.57 MeV and 13.75 MeV neutrons energies (ii) out of five values of cross sections reported by Kasugai and Ikeda (1997) three values of cross sections at 13.70,14.03 and 14.95 MeV at neutron energies, and (iii) out of six values of cross sections reported by Sakane et al. (2001), four values of cross sections at 13.65,13.88,14.28 and 14.58 MeV neutron energies are covered under the seven plots of theoretical cross sections estimated by EMPIRE 3.2 –LEVEDEN 4 with parameters of GSTRFN from 0 to 6 (Kopecky et al., 1993; Mughabghab and Dunford, 2000; Plujko, 2000) over 10–20 MeV neutron energy range. It is observed that when two additional plots of cross sections estimated by EMPIRE-3.2 using LEVDEN Default 0 & 1 parameters were added in Fig. 3,all the experimental cross sections reported in literature (Reyhancan et al., 2003; Sakane et al., 2001; Kasugai and Ikeda, 1997) could be encompassed under nine plots of theoretical cross sections shown in Fig. 3.

Fig. 4 shows two selective plots of cross sections, one plot is of TALYS-1.8 with ldmodel 5, preequilibrium, preeqmode 4 parameters, and the other plot is of EMPIRE-3.2 with LEVDEN 4, GSTRFN 0 parameters obtained respectively from Fig. 2 and Fig. 3. The cross sections measured in the present work at five neutron energies 13.73 MeV, 14.07 MeV, 14.42 MeV, 14.68 MeV and 14.77 MeV match fairly well, within experimental error, with the TALYS 1.8 and EMPIRE3.2 plots shown in Fig. 4.Moreover,in the present work the observed increase in the cross sections with neutron energy, over 13.73–14.77 MeV, is consistent with the corresponding theoretical cross- sections.

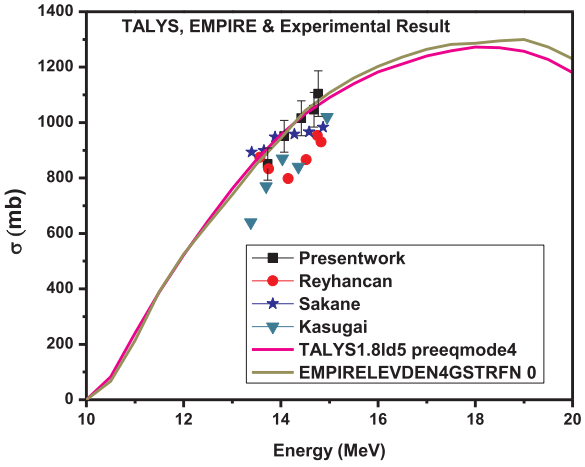

Fig. 4. Comparison of cross sections of ^{140}Ce(n, 2n)^{139m}Ce reaction(i) theoretically estimated over 10–20 MeV neutron energy range using EMPIRE-3.2 –LEVEDEN 4 with parameters of GSTRFN 0 (Kopecky et al., 1993) and TALYS-1.8 ld model 5 (Goriely et al., 2008, 2001) with the cross sections (i)measured in the present work at 13.73 MeV 14.07 MeV, 14.42 MeV, 14.68 MeV and 14.77 MeV neutron energies and (ii) reported in literature (Reyhancan et al., 2003; Sakane et al., 2001; Kasugai and Ikeda, 1997).

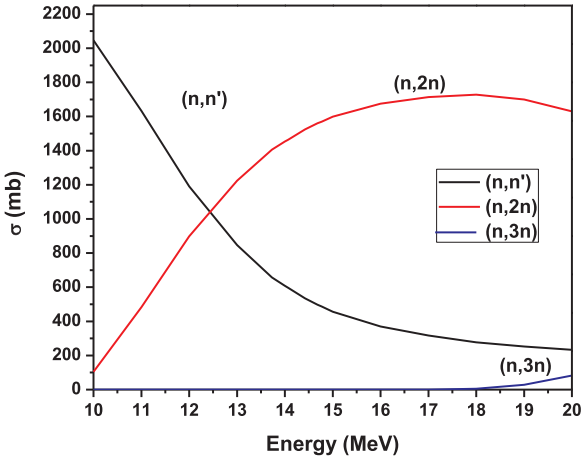

Fig. 5. Theoretical cross sections of ^{140}Ce (n, n′) ^{140}Ce*, ^{140}Ce(n, 2 n)^{139}Ce and ^{140}Ce (n, 3 n) ^{138}Ce reactions estimated using TALYS 1.8 over 10–20 MeV neutron energy range.

By comparing the cross sections reported in literature (Reyhancan et al., 2003; Sakane et al., 2001; Kasugai and Ikeda, 1997) with the

theoretical plots in Fig. 5,it is observed that (i) five out of six cross sections measured byReyhancan et al.,(2003), (ii) all the five cross sections measured by Kasugai and Ikeda (1997)and (iii) four out of six cross sections measured by Sakane et al. (2001)do not match with the theoretical plots of TALYS 1.8 and EMPIRE 3.2.

Fig. 5 shows that the cross section for (n, n′) reaction decreases continuously with the increase in the neutron energy over 10–20 MeV range, and attributed to the increase in the (n, 2n) cross sections. However, it is interesting to note that the cross section of (n, n′) reaction is relatively large ~2000 mb at 10 MeV neutrons, and even has appreciable value, varying from around 600–500 mb over 14–15 MeV neutron energy range.

Furthermore, the cross section of ^{140}Ce(n, 2n)^{139}Ce increases over the neutron energy range of 10 MeV to around 17 MeV, and then gradually decreases with the further increase in the neutron energy.The decrease in the (n, 2n) cross section is attributed to the initiation of (n, 3n) reaction channel having threshold energy ~16.77 MeV. However, this trend is a general feature for (n, 2n) and (n, 3n) reactions for any nucleus.

5. Conclusions

The cross sections for formation of ^{139m}Ce through the ^{140}Ce(n, 2n)^{139m}Ce reaction were measured at five different neutron energies, over 13.73–14.77 MeV range. The corresponding cross-sections over 10–20 MeV neutron energy range were also estimated using the TALYS 1.8 and EMPIRE-3.2 codes, with different input parameters. In the present work, the cross sections of ^{140}Ce(n, 2 n)^{139m}Ce reaction measured at five neutron energies show good matching, within experimental error bars, with the single theoretical cross sections estimated by EMPIRE 3.2 –LEVEDEN 4 with GSTRFN from 1–6 parameters as well as that estimated by TALYS 1.8 using preequilibrium, preeqmode 4 and level density model 1–6 parameters.

For this reactions, three sets of cross sections over five to six neutron energies in the range of 13–15 MeV are reported in literature (Reyhancan et al., 2003; Sakane et al., 2001; Kasugai and Ikeda, 1997).However, the cross sections of any single set could not lie on any one single theoretical plot of cross-sections estimated by TALYS 1.8 and EMPIRE-3.2 codes in the present work. For this reaction, the cross sections measured in the present work at five neutron energies over the over 13.73–14.77 MeV range show good matching with the theoretical cross sections. Moreover, the theoretical cross sections for formation of metastable state, ^{139m}Ce, increases over 10 MeV to ~ 17 MeV neutron energy range.These results are also consistent because the minimum neutron energy required to excite the ^{139}Ce nucleus to 1.3202 MeV energy level, just above the metastable state level is close to 10 MeV, and maximum neutron energy~ 17 MeV is below the threshold of (n, 3 n) reaction.

Acknowledgements

One of the authors, Vishal Bharud, is thankful to Dr. Babasaheb Ambedkar Research and Training Institute, Government of Maharashtra, Pune, India for the award of SRF. Similarly, the corresponding author V.N. Bhoraskar is grateful to the authorities of Savitribai Phule Pune University, Pune, for the nomination as Distinguished Professor. Nuclear Data and other information provided by Dr. N. Otsuka, International Atomic Energy Agency, Vienna International Centre, Austria, is gratefully acknowledged. The help in the experimental work and theoretical calculations extended by Dr. B.J. Patil, Avinash Deore, Ashish Thorat, Ambadas Phatangare and Gaurav Bholane of the Department of Physics is acknowledged. The authors would like to express sincere thanks to Dr. B. Lalremruata of Mizoram university for discussions as well as for providing scientific information and technical data required for the present work.

References

Attar, F.M.D., Mandal, R., Dhole, S.D., Saxena, A., Ashokkumar, Ganesan, S., Kailas, S., Bhoraskar, V.N., 2008. Cross-sections for formation of ^{89}Zr^{m} through ^{90}Zr(n, 2n)^{89}Zr^{m} reaction over neutron energy range 13.73 MeV to 14.77 MeV. Nucl. Phys. A 802, 1–11. https://doi.org/10.1016/j.nuclphysa.2008.01.010.

Attar, F.M.D., Dhole, S.D., Bhoraskar, V.N., 2014. Cross sections of the (n, p) reaction on the ^{78}Se and ^{80}Se isotopes measured for 13. 73 MeV to 14. 77 MeV and estimated for 10 MeV to 20 MeV neutron energies. Phys. Rev. C 064609, 1–9. https://doi.org/10.1103/PhysRevC.90.064609.

Badwar, S., Ghosh, R., Lawriniang, B.M., Vansola, V., Gopalakrishna, A., Naik, H., Naik, Y., Suryanarayana, S.V., Salunkhe, S.Y., Agarwal, A., Ware, S., Gupta, A.K., Jyrwa, B., Ganesan, S., Singh, P., Goswami, A., 2016. ^{151}Eu(n,γ)^{152m1}Eu reaction cross-section measurement at the neutron energies of 1.12, 2.12, 3.12 and 4.12 MeV. J. Radioanal. Nucl. Chem. 307, 1385–1390. https://doi.org/10.1007/s10967-015-4230-2.

Barough, M.S., Patil, B.J., Bhoraskar, V.N., Dhole, S.D., 2014. Measurement and estimation of isomeric cross section of ^{137}Ba(n, n′)^{137m}Ba reaction using accelerator based neutron source. Ann. Nucl. Energy 63, 209–214. https://doi.org/10.1016/j.anucene.2013.07.032.

Basunia, M.S., 2011. Nuclear data sheets for A = 27 *. Nucl. Data Sheets 112, 1875–1948. https://doi.org/10.1016/j.nds.2011.08.001.

Berglund, M., Wieser, M.E., 2011. Isotopic compositions of the elements 2009 (IUPAC Technical Report)* 83, 397–410. https://doi.org/10.1351/PAC-REP-10-06-02.

Bramlitt, E.T., Fink, R.W., 1963. Rare nuclear reactions induced by 14.7-MeV neutrons. Phys. Rev. 131, 2649–2663.

Capote, R., Herman, M., Obložinský, P., Young, P.G., Goriely, S., Belgya, T., Ignatyuk, A.V., Koning, A.J., Hilaire, S., Plujko, V.A., Avrigeanu, M., Bersillon, O., Chadwick, M.B., Fukahori, T., Ge, Z., Han, Y., Kailas, S., Kopecky, J., Maslov, V.M., Reffo, G., Sin, M., Soukhovitskii, E.S., Talou, P., 2009. RIPL - reference input parameter library for calculation of nuclear reactions and nuclear data evaluations. Nucl. Data Sheets 110, 3107–3214. https://doi.org/10.1016/j.nds.2009.10.004.

ENDF/B-VII.1, 2018. National Nuclear data center, Brookhaven National Laboratory.

EXFOR, 2013. Experimental Nuclear Reaction data. IAEA.

Filtankov A.A., 2016. USSR reported to the I.N.D.C. No. 0460.

Gardner, D.G., 1984. Neutron Radiative Capture, OECD/NEA Series on Neutron Physics and Nuclear Data in Science andTechnology. eds. A. Michaudon al., 62.

Goriely, S., Tondeur, F., Pearson, J.M., 2001. A Hartree–Fock Nuclear Mass Table. At. Data Nucl. Data Tables 77, 311–381. https://doi.org/10.1006/adnd.2000.0857.

Goriely, S., Hilaire, S., Koning, A.J., 2008. Improved microscopic nuclear level densities within the Hartree-Fock-Bogoliubov plus combinatorial method. Phys. Rev. C - Nucl. Phys. 78, 1–14. https://doi.org/10.1103/PhysRevC.78.064307.

Hauser, W., Feshbach, H., 1952. The inelastic scattering of neutrons. Phys. Rev. 87, 366–373. https://doi.org/10.1103/PhysRev.87.366.

Herman, M., Capote, R., Sin, M., Trkov, A., Carlson, B.V., Obložinský, P., Mattoon, C.M., Wienke, H., Hoblit, S., Cho, Y., Nobre, G.P.A., Plujko, V.A., Zerkin, V., 2013. EMPIRE-3.2 Malta Modular system for nuclear reaction calculations and nuclear data evaluation. Indc(Nds)-0603 14, 1–299 (Bnl-101378-2013).

Hilaire, S., Girod, M., Goriely, S., Koning, A.J., 2012. Temperature-dependent combinatorial level densities with the D1M Gogny force. Phys. Rev. C - Nucl. Phys. 86, 1–10. https://doi.org/10.1103/PhysRevC.86.064317.

Jagtap, A.S., Palani, T., Patil, B.J., T, C.S., Pethe, S.N., Kulkarni, G., Bhoraskar, V.N., Dhole, S.D., 2016. Monte Carlo based investigations of electron contamination from telecobalt unit head in build up region and its impact on surface dose. Appl. Radiat. Isot. 118, 175–181. https://doi.org/10.1016/j.apradiso.2016.09.012.

Joshi, P.K., Singh, B., Singh, S., Jain, A.K., 2016. Nuclear Data Sheets for A = 139*. Nucl. Data Sheets 138, 1–292. https://doi.org/10.1016/j.nds.2016.11.001.

Kasugai, Y., Ikeda, Y.U, Y., 1997. Activation cross section measurements for La, Ce, Pr, Nd, Gd, Dy and Er isotopes by 14 MeV neutrons,In: Proceedings of the Conference on Nuclear Data for Science and Technology, Trieste, Italy. p. 635.

Katalenich, J.A., Hartman, M.R., Brien, R.C.O., Howe, S.D., 2013. Fabrication of cerium oxide and uranium oxide microspheres for space nuclear power applications. Nucl. Emerg. Technol. Sp. 2013.

Kestelman, A.J., Ribeiro Guevara, S., Arribére, M.A., Cohen, I.M., 2007. Averaged cross sections for the reactions 68Zn(n,p)68gCu and 68Zn(n,p)68mCu for a 235U fission neutron spectrum. Appl. Radiat. Isot. 65, 872–876. https://doi.org/10.1016/j.apradiso.2007.03.008.

Kong, X., Wang, Y., Yang, J., 1998. Cross sections for (n, 2n), (n, p) and (n, a) reactions on rare-earth isotopes at 14. 7 MeV. Appl. Radiat. Isot. 49, 1529–1532.

Koning, A., Hilarie, S., Goriely, S., 2015. Talys-1.8 a nuclear reaction program. Nucl. Data Sect.

Koning, A.J., Delaroche, J.P., 2003. Local and global nucleon optical models from 1 keV to 200 MeV. Nucl. Phys. A 713, 231–310.

Kopecky, J., 1817. n.d. Recommended Gamma Ray Strength Functions. ECN P.O.Box 1, 1755 ZG Petten JUKO Res HX Alkmaar, Netherlands, Priv. Commun. 119–133.

Kopecky, J., Uhl, M., Chrien, R.E., 1993. Radiative strength in the compound nucleus 157Gd. Phys. Rev. C 47, 312–322.

Lalremruata, B., Dhole, S.D., Ganesan, S., Bhoraskar, V.N., 2009. Excitation function of the ^{93}Nb(n,2n)^{92}Nb^{m} reaction from threshold to 24 MeV. Phys. Rev. C 80, 014608. https://doi.org/10.1103/PhysRevC.80.014608.

Lalremruata, B., Otuka, N., Tambave, G.J., Mulik, V.K., Patil, B.J., Dhole, S.D., Saxena, A., Ganesan, S., Bhoraskar, V.N., 2012. Systematic study of (n, p) reaction cross sections from the reaction threshold to 20 MeV. Phys. Rev. C 024624, 1–13. https://doi.org/10.1103/PhysRevC.85.024624.

Luo, J., Xu, X., Cao, X., Kong, X., 2007. Activation cross sections and isomeric cross section ratios for the (n,2n) reactions on ^{175}Lu, ^{198}Pt and ^{82}Se from 13.5 to 14.6 MeV.

Nucl. Instrum. Methods Phys. Res. Sect. B Beam Interact. Mater. At. 265, 453–460. https://doi.org/10.1016/j.nimb.2007.10.005.
Luo, J., Wang, X., Liu, Z., Tuo, F., Kong, X., 2009. Activation cross-sections for ^{158}Dy (n,p)^{158}Tb, ^{156}Dy(n,a)^{153}Gd and ^{160}Dy(n,p)^{160}Tb reactions induced by neutrons at 14.7 MeV. Appl. Radiat. Isot. 67, 1892–1896. https://doi.org/10.1016/j.apradiso.2009.05.013.
Luo, J., An, L., Jiang, L., 2015. Neutron-induced activation cross-sections on natural cerium up to 20 MeV. J. Radioanal. Nucl. Chem. 305, 691–700. https://doi.org/10.1007/s10967-015-4049-x.
Mughabghab, S.F., Dunford, C.L., 2000. A dipole – quadrupole interaction term in E1 photon transitions. Phys. Lett. B 487, 155–164.
Naik, H., Kim, G.N., Schwngner, R., Kim, K., Goswami, A., 2013. Photoneutron reaction cross section for ^{93}Nb in the end-point bremsstrahlung energies of 12-16 and 45–70 MeV. Nucl. Phys. A 916, 168.
Naylor, H., White, R.E., 1977. An accurate measurement of the ^{27}Al(p,n)^{27}Si threshold energy. Nucl. Instrum. Methods 144, 331–335. https://doi.org/10.1016/0029-554X(77)90125-2.
Otuka, N., Smith, D.L., 2014. Documentation of uncertainties in experimental cross sections for EXFOR (IAEA-EXFOR Database). Nucl. Data Sheets 120, 281–284.
Otuka, N., Lalremruata, B., Khandaker, M.U., Usman, A.R., Punte, L.R.M., 2017. Uncertainty propagation in activation cross section measurements. Radiat. Phys. Chem. 140, 502–510. https://doi.org/10.1016/j.radphyschem.2017.01.013.
Pandey, B., Agrawal, H.M., Pepelnik, R., 2014. Neutron activation cross-sections for ytterbium isotopes at (14.6 ± 0.3)mev. Appl. Radiat. Isot. 85, 128–132. https://doi.org/10.1016/j.apradiso.2013.11.114.
Parashari, S., Mukherjee, S., Vansola, V., Makwana, R., Singh, N.L., Pandey, B., 2018. Investigation of (n, p), (n, 2n) reaction cross sections for Sn isotopes for fusion reactor applications. Appl. Radiat. Isot. 133, 31–37. https://doi.org/10.1016/j.apradiso.2017.12.003.
Patil, B.J., Chavan, S.T., Pethe, S.N., Krishnan, R., Dhole, S.D., 2010. Measurement of angular distribution of neutron flux for the 6 MeV race-track microtron based pulsed neutron source. Appl. Radiat. Isot. 68, 1743–1745. https://doi.org/10.1016/j.apradiso.2010.04.020.
Patil, B.J., Chavan, S.T., Pethe, S.N., Krishnan, R., Bhoraskar, V.N., Dhole, S.D., 2012. Design of 6 Mev linear accelerator based pulsed thermal neutron source: FLUKA simulation and experiment. Appl. Radiat. Isot. 70, 149–155. https://doi.org/10.1016/j.apradiso.2011.08.019.
Plujko, V.A., 2000. A new closed-form thermodynamic approach for radiative strength functions. Acta Phys. Pol. B 31, 435.
Qaim, S.M., 1974. Total (n, 2n) cross sections and isomeric cross section ratios at 14.7 MeV in the region of rare earths. Nucl. Phys. A 224.
Reyhancan, I.A., Bostan, M., Durusoy, A., 2003. Measurements of isomeric cross sections for (n, 2n) reaction on ^{140}Ce, ^{142}Nd and ^{144}Sm isotopes around 14 MeV. Ann. Nucl. Energy 30, 1539–1547. https://doi.org/10.1016/S0306-4549(03)00100-2.
RNAL, 2002. Reference neutron activation library, IAEA-TECDOC-1285, April.
Rosman, K.J., Taylor, P.D.P., 1998. ELemental isotpes Compositions of the elements 1997. J. Phys. Chem. Ref. Data 27, 1275–1287.
Şahan, M., Tel, E., Şahan, H., Gevher, U., Kara, A., 2016. Cross section calculations of (n,2n) and (n,p) nuclear reactions on germanium isotopes at 14–15 MeV. J. Fusion Energy 35, 730–742. https://doi.org/10.1007/s10894-016-0101-2.
Sakane, H., Kasugai, Y., Shibata, M., Iida, T., Takahashi, A., Fukahori, T., Kawade, K., 2001. Measurement of activation cross-sections for (n, 2n) reactions producing short-lived nuclei in the energy range between 13.4 and 14.9 MeV. Ann. Nucl. Energy 28, 1175–1192.
Sarkar, R., Bhoraskar, V.N., 1992. Cross sections for formation of metastable states of ^{79}Br, ^{90}Zr, and ^{95} Tc nuclei at 14 MeV neutron energy. Phys. Rev. C. 46, 2246–2250.
Sarkar, R., Bhoraskar, V.N., 1998. Spin distribution factor for formation of metastable states of ^{90}Y and ^{91}Y through (n,p) reactions over neutron energies 5–15 MeV. Nucl. Phys. A 633, 640–650.
Satoh, Y., Matsumoto, T., Kasugai, Y., Yamamoto, H., Iida, T., Takahashi, K.K, A., 1995. Measurement of formation cross section producing short-lived nuclei by 14 MeV neutrons - Na, Si, Te,Ba, Ce, Sm,W,Os, In: JAERI Conference Proceedings, Japan. p. 189.
Semkova, V., Avrigeanu, V., Glodariu, T., Koning, A.J., Plompen, A.J.M., Smith, D.L., Sudár, S., 2004. A systematic investigation of reaction cross sections and isomer ratios for neutrons up to 20 MeV on Ni-isotopes and ^{59}Co by measurements with the activation technique and new model studies of the underlying reaction mechanisms. Nucl. Phys. A 730, 255–284. https://doi.org/10.1016/j.nuclphysa.2003.11.005.
Taylor, John R., 1939. An Introduction to Error Analysis 1982 University Science Books, Mill Valley.
Torrel, S., Krane, K.S., 2012. Neutron capture cross sections of ^{136,138,140,142}Ce and the decays of ^{137}Ce. Phys. Rev. C. 86, 034340. https://doi.org/10.1103/PhysRevC.86.034340.
Van Gosen, B.S., Verplanck, P.L., Long, K.R., Gambogi, J., Seal II, R.R., 2014. The rare-earth elements — vital to modern technologies and lifestyles. US Geol. Surv. Fact. Sheet 2014–3078, 4. https://doi.org/10.3133/fs20143078.
Vogt, K., Mohr, P., Babilon, M., Bayer, W., Galaviz, D., Hartmann, T., Hutter, C., Rauscher, T., Sonnabend, K., Volz, S., Zilges, A., 2002. Measurement of the (gamma, n) cross section of the nucleus Au-197 close above the reaction threshold. Nucl. Phys. A 707, 241–252.
Wille, R.G., Fink, R.W., 1960. Activation cross sections for 14.8-Mev neutrons and some new radioactive nuclides in the rare earth region. Phys. Rev. 118, 242–248.
Yiğit, M., 2018. Analysis of (n,p) cross sections near 14 MeV. Appl. Radiat. Isot. 135, 115–122. https://doi.org/10.1016/j.apradiso.2018.01.029.
Yoshimi, Kasugai, Hiroshi, Yamamoto, K.K, T.I, 1998. Measurement of (n, p) cross-sections for short lived products by 13. 4–14.9 MeV neutrons. Ann. Nucl. Energy 25, 23–45.